Applied Physics Letters

Self-assembled single-digit nanometer memory cells

Cite as: Appl. Phys. Lett. **113**, 062404 (2018); https://doi.org/10.1063/1.5033972
Submitted: 08 April 2018 • Accepted: 25 July 2018 • Published Online: 09 August 2018

J. Hong, K. Dong, J. Bokor, et al.

AIP Publishing

Self-assembled single-digit nanometer memory cells

J. Hong,[1,a)] K. Dong,[2] J. Bokor,[3] and L. You[1,a)]
[1]School of Optical and Electronic Information, Huazhong University of Science and Technology, Wuhan 430074, People's Republic of China
[2]Department of Automation, China University of Geosciences, Wuhan 430074, People's Republic of China
[3]EECS, University of California-Berkeley, Berkeley, California 94720, USA

(Received 8 April 2018; accepted 25 July 2018; published online 9 August 2018)

The current spintronic research focuses on lowering switching energy and maintaining good thermal stability of nanomagnets, which could ensure further development of memory technology. Here, we investigate a single-digit nanometer magnetic tunnel junction composed of self-assembled FePt nanopillars isolated by crystallized ZrO_2. We find that the lateral size range of the operational device could be sub-7-nm by maintaining outstanding thermal stability. *Published by AIP Publishing.*
https://doi.org/10.1063/1.5033972

The demand for high density and high performance nonvolatile memory has increased drastically over the past decade as the market for consumer electronics has expanded.[1] Spin transfer torque magnetic random access memory (STT-MRAM) using a magnetic tunnel junction (MTJ) with perpendicular magnetic anisotropy (PMA) is one of the most promising nonvolatile memory technologies.[2–6] It combines a unique set of advantages such as quasi-infinite write endurance, high speed, low power consumption, and scalability.[7,8] The key issues of STT-MRAM include the relatively high current density of spin-torque switching and the low thermal stability factor of the bit cell. The thermal stability factor Δ above 60 is required for the data retention time of stored information to extend beyond 10 years when the magnetization direction is just sufficiently high enough to store the magnetization.[9–13]

In the past decade, there has been significant amount of research in the field of MTJs with PMA (pMTJ). The crystallized pMTJs with CoFeB/MgO has shown a tunneling magnetoresistance (TMR) ratio of more than 100%. The film structures also exhibit high thermal stability and low switching current density. The thermal stability of magnetization is important to store the information for longer periods without self-erasure. The thermal stability factor Δ is defined by E_B/k_BT, where E_B is the energy barrier. The energy barrier is written as $K_{eff}V$, where K_{eff} is the effective magnetic anisotropy and V is the volume. K_{eff} $(=K_u + K_i/t + K_d)$ is divided into three terms: K_u, K_i, *and* K_d, respectively. K_u is the possible uniaxial magneto-crystalline or magneto-elastic anisotropy (negligible in the case of pMTJs). The positive interfacial anisotropy K_i switches the magnetization direction of a very thin film (usual thickness $t < 2$ nm) in the out-of-plane direction as the negative demagnetization anisotropy K_d would usually keep the magnetization within the plane as the thickness is much lower than the diameter (>20 nm). Therefore, pMTJs with CoFeB/MgO are not allowed to scale down to less than 20 nm even using the double-interface (Co)FeB-MgO MTJ since the effective perpendicular anisotropy energy dominated by interfacial anisotropy reaches a physical limit of providing sufficient thermal stability.[14] However, some research showed very low switching energy when the pMTJ scales down to single-digit nm range with low thermal stability and opened a new avenue to sub-10-nm pMTJs.[15,16]

Recent reports including Watanabe *et al.* and Perissin *et al.* independently proposed the storage layer with very thick ferromagnets such as FeB and Co(NiFe) producing positive shape anisotropy to maintain the thermal stability factor over 60 for single-digit nm pMTJs.[17,18] The remaining issue for the fabrication is that the structures need to be patterned by electronic beam lithography followed by sophisticated ion beam etching (IBE) or reactive ion etching (RIE). $L_{1(0)}$-ordered FePt (100) structures with ultrahigh anisotropy allow thermally stable grain sizes down to sub-3-nm. The FePt-based single-digit nm structure has been achieved by several ways such as bit patterned magnetic media (BPM),[19,20] self-assembled growth, and some others. However, BPM also involve a sophisticated lithography process.

Here, we present an approach to achieve a sub-7-nm memory cell with PMA, which is obtained by growing nanostructured columns of $L_{1(0)}$ ordered FePt grains (the smallest lateral sizes are around 5 nm ± 2 nm diameter) isolated by doping a tetragonal (002) textured oxide, ZrO_2. The doped oxide was distributed at the grain boundaries of FePt grains. The structure was obtained by virtue of self-assembled growth co-sputtering from the targets of a $Fe_{55}Pt_{45}$ alloy and ZrO_2 at high temperatures. The memory cell is read by probe-induced spin polarized currents. The self-assembled single-digit nm perpendicular nanomagnets (SAPN) with good thermal stability factor based on probe-based MTJs (SAPN-STT-MRAM) open a new path towards next generation of STT-MRAM with ultra-high density, outstanding thermal stability, and low power consumption.

Figure 1(a) shows an exaggerated schematic of a self-assembled FePt structure. The microstructure achieved in the FePt-ZrO_2 composites was very close to that required for practical applications. A critical issue was required to be resolved: columnar shaped FePt grains with the aspect ratio of $h/D > 1$ where h is the height and D is the diameter of the self-assembled structures. Different sputtering conditions resulted in a FePt-ZrO_2 film to form different microstructure of the composites. Crystallized ZrO_2 distributed at the grain boundary of FePt grains and columnar structured FePt grains

a)Electronic addresses: jeongmin.hong@gmail.com and lyou@hust.edu.cn

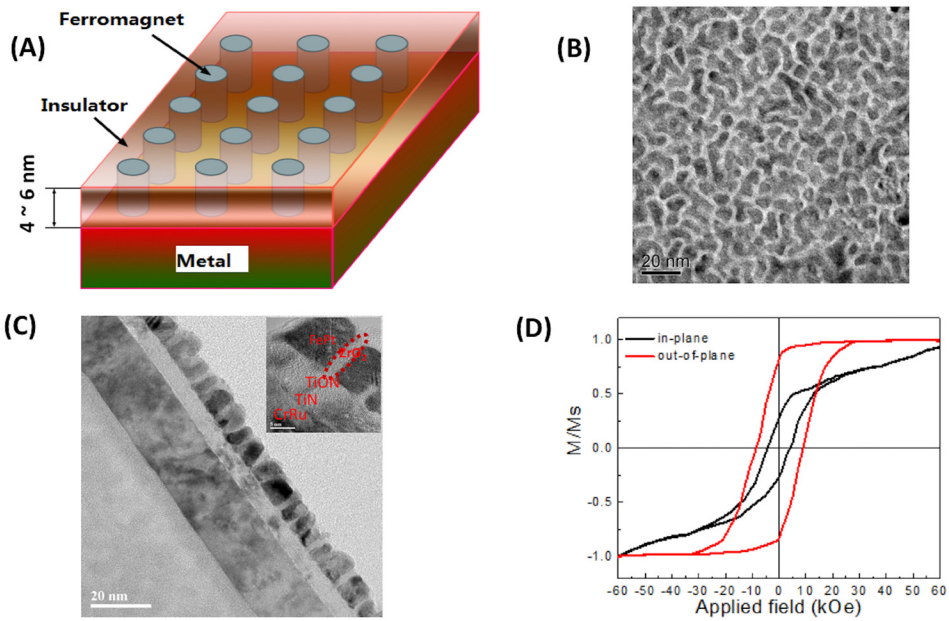

FIG. 1. Self-assembled growth of FePt pillars with PMA. (a) Schematic of a self-assembled FePt structure. (b) SEM image of the single-digit nm pillar structure. (c) TEM image of the structure. (d) M-H loops of the same structure.

were achieved. As shown in Fig. 1(b), crystallized FePt(001) columnar structures were maintained and the well isolated FePt grains with a columnar structure were achieved. A TEM image of the final structures is shown in Fig. 1(c). The columnar structured FePt grains were formed with the increase in FePt thickness from 4 to 6 nm. Here, the thickness was 4 nm and Fig. 1(c) shows the optimal multi-layered thin film stack of glass/CrRu/TiN/TiON/FePt-ZrO_2.

Figure 1(d) confirms that it exhibits strong PMA with an out-of-plane coercivity of 23.2 kOe and the anisotropy field in the hard axis shows about 6T. The anisotropy K_u is estimated to be around 3.0×10^7 erg/cc. For example, commercially available magnetic devices in hard disk drive media are required to have higher K_u and very small grain size down even to sub-3-nm. This is in well agreement with the grown structure in Fig. 1.

The magnetic thin film deposited functional nanoprobe was fabricated. State-of-the-art He-ion focused ion beam (He-FIB) trimming was performed to fabricate the smallest possible structure. As shown in Fig. 2(a), the MTJ system configurations are described. Each magnet could switch the magnetization direction through spin-polarized currents. Depending on the orientations of the magnets, the junction structure showed parallel (P) and anti-parallel (AP) states.

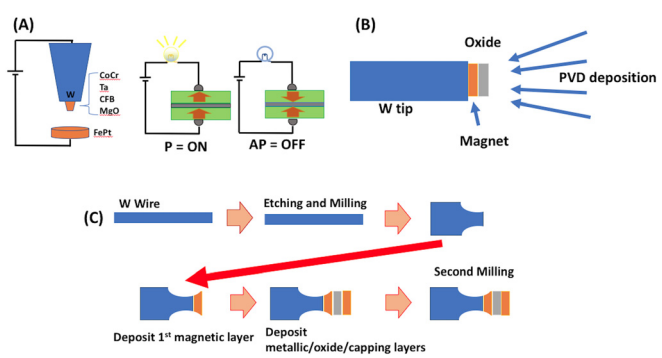

FIG. 2. STM probe fabrication with Ta/CoFeB/MgO stacks. (a) Concept of the device. (b) Schematic of the probe. (c) Step-by-step fabrication process of the probe.

A nanoscale multilayered thin-film stack on top of the tip was deposited and the fabrication process of the probe was performed from the tip milling to deposit several magnetic thin-films with an insulation layer as illustrated in Fig. 2(b). From the pristine W wire, the tip was etched and milled several times. A multilayered thin-film stack was deposited on top of the probes afterwards. The standard stack of CoCr(10 nm)/Ta(5 nm)/CoFeB(1 nm)/MgO(0.9 nm) on the W tip side was deposited. The developed fabrication process of the probe used in this study is shown in Fig. 2(c).

Figure 3(a) shows the grown $L_{1(0)}$-ordered FePt nanostructure. The substrate contains several different size ranges of the magnets, but the maximum size is about 10 nm. STM measurements are done via current mode to distinguish the density of state (DOS) through magnets. The structure was perpendicularly magnetized in one direction and imaging was performed. Then, it was magnetized in the other direction before another imaging was performed.

The STM image on top right in Fig. 3(a) displays the resulting images after applying the magnetic field on either negative or positive side above the switching magnetic field of the substrate. Two images on the top left side in Fig. 3(a)

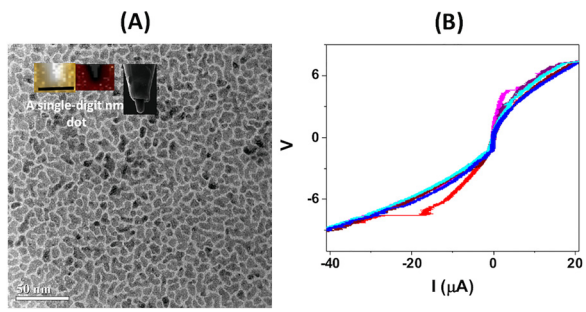

FIG. 3. Self-assembled single-digit nm perpendicular nanomagnet (SAPN) STT-MRAM. (a) Sub-7-nm L1(0)-ordered FePt structure. Top left inset shows magnetization switching of nanomagnets as read by functional STM tips. Bright and dark colors indicate two distinctive magnetization switching. The scale bar is 10 nm. (b) I-V curves recorded via sweeping the voltage by changing the magnetic field. Red and purple lines show I-V curves recorded without a magnetic field.

are current variation (density of states mode) images from the measurement. While sweeping the voltage, the single-digit nm (~7 nm) media clearly switch the direction of magnetization as shown in Fig. 3(a).

To test the *I-V* characteristics, we performed transport measurements built in a STM setup. During the measurement, it was gently engaged to the substrate with high current (point-contact mode). The *I-V* curve shows hysteretic behavior which contains "P" and "AP" states. As shown in Fig. 3(b), red and purple lines exhibit current jumps at constant voltage. The jumps come from the "AP" state of magnets. When the magnetic field was applied, the "AP" state disappeared. The result clearly presents the field dependence of *IV* characteristics of the device.

There are three findings in this work: (1) a self-assembled single-digit nm FePt nanostructure was synthesized. The pillars reached down to less than 5 nm range. (2) The fabrication of a magnetic probe was demonstrated. (3) Point contacts induced magnetization switching was demonstrated followed by previous works.[16] The magnetization switching of the material with high thermal stability was achieved. In summary, the prototype of the device could be used to memory applications without involving any complicated patterning process such as e-beam lithography, RIE, and IBE. The proposed SAPN-STT-MRAM is also significant because it could be further scaled down to sub-7-nm memory bit with high thermal stability Δ. The calculated thermal stability factor of SAPN-STT-MTJ is over 85.

For obtaining the self-assembled single-digit nm memory cell, FePt (2–6 nm)−35 vol. % of ZrO_2/TiON (2 nm)/TiN (3 nm)/CrRu (30 nm) was grown at 800 K by a magnetron sputtering system with a base pressure of 2×10^{-8} Torr. All the FePt-ZrO_2 layers were deposited by co-sputtering of a $Fe_{55}Pt_{45}$ alloy and ZrO_2 with 10 mTorr of Ar gas flow. After the process, the sample was cooled down to room temperature.

Using probe-based electronics, there are many opportunities to develop future electronics. Probe based electronics have been firstly developed for the use of memory and storage applications.[21,22] In spintronics, many state-of-the-art technologies have been established to show a simple prototype with device physics based on the probe based systems.[16,23,24] Recently, single-digit nm MTJ prototypes with the manipulation of a nano-probe have been reported.[16]

For the probe fabrication, CoFeB magnets and MgO insulation layers were deposited through the sputtering system which has the base pressure of $\sim 2.0 \times 10^{-8}$ Torr and a process pressure range from 1.8×10^{-3} Torr to 5×10^{-3} Torr. The annealing temperature has been increased up to 800 K. An ultrahigh-quality and high-density MgO target was used and the process pressure, gas flow, power, and time have been optimized for the deposition of ideal structures. The state-of-the-art He ion focused ion beam was used to trim the final structure as reported in other works.[15,25]

High sensitive MOKE measurements were performed using a home-made focused MOKE system. A 635-nm diode laser was directed toward the sample, which was located between the poles of a vector magnet. The magnetic field at the probe spot was calibrated by a three-axis Hall probe sensor (C-H3A-2m Three Axis Magnetic Field Transducer, SENIS GmbH Zürich, Switzerland). The accuracy of the magnetic field measurement is estimated to be at ~1%. The time to sweep full hysteresis loops was 20 min (5 Oe/s).

Scanning tunneling microscopy (STM) was performed in contact mode (high current mode to modulate the distance between the probe and substrates) using a Bruker-Nano AFM system. The ultra-high sensitivity magnetic tip was fabricated. The dynamics were measured in the presence of a magnetic field by sweeping the magnetic field range in perpendicular direction.

Programmable transport measurement was made with a home-made measurement set up which could perform high sensitivity point contact transport measurements. The sample was mounted on a chip carrier after wire bonded carefully and inside a Faraday cage to reduce possible noises during the measurement.

This work was supported by the National Natural Science Foundation of China under Award No. 61674062 and by the U.S. Department of Energy, Office of Basic Energy Sciences, Division of Materials Sciences and Engineering under Contract No. DE-AC02-05CH11231. The authors acknowledge the financial support from the National Science Foundation (NSF) Center for Energy Efficient Electronics Science (E3S) under Award No. 0939514.

[1]L. Thomas, G. Jan, J. Zhu, H. Liu, Y.-J. Lee, S. Le, R.-Y. Tong, K. Pi, Y.-J. Wang, D. Shen, R. He, J. Haq, J. Teng, V. Lam, K. Huang, T. Zhong, T. Torng, and P.-K. Wang, "Perpendicular spin transfer torque magnetic random access memories with high spin torque efficiency and thermal stability for embedded applications," J. Appl. Phys. **115**(17), 172615–172616 (2014).
[2]M. Julliere, "Tunneling between ferromagnetic films," Phys. Lett. A **54**(3), 225–226 (1975).
[3]T. Miyazaki and N. Tezuka, "Giant magnetic tunneling effect in Fe/Al2O3/Fe junction," J. Magn. Magn. Mater. **139**(3), L231–L234 (1995).
[4]J. S. Moodera, L. R. Kinder, T. M. Wong, and R. Meservey, "Large magnetoresistance at room temperature in ferromagnetic thin film tunnel junctions," Phys. Rev. Lett. **74**(16), 3273–3276 (1995).
[5]J. C. Slonczewski, "Currents and torques in metallic magnetic multilayers," J. Magn. Magn. Mater. **247**, 324–329 (2002).
[6]S. Ikeda, J. Hayakawa, Y. Ashizawa, Y. M. Lee, K. Miura, H. Hasegawa, M. Tsunoda, F. Matsukura, and H. Ohno, "Tunnel magnetoresistance of 604% at 300 K by suppression of Ta diffusion in CoFeB/MgO/CoFeB pseudo-spin-valves annealed at high temperature," Appl. Phys. Lett. **93**, 082508 (2008).
[7]S.-W. Chung, T. Kishi, J. W. Park, M. Yoshikawa, K. S. Park, T. Nagase, K. Sunouchi, H. Kanaya, G. C. Kim, K. Noma, M. S. Lee, A. Yamamoto, K. M. Rho, K. Tsuchida, S. J. Chung, J. Y. Yi, H. S. Kim, Y. S. Chun, H. Oyamatsu, and S. J. H, "4Gbit density STT-MRAM using perpendicular MTJ realized with compact cell structure," in *IEEE IEDM* (2016), pp. 659–662.
[8]B. Dieny and M. Chshiev, "Perpendicular magnetic anisotropy at transition metal/oxide interfaces and applications," Rev. Mod. Phys. **89**, 25008 (2017).
[9]S. Ikeda, K. Miura, H. Yamamoto, K. Mizunuma, H. D. Gan, M. Endo, S. Kanai, J. Hayakawa, F. Matsukura, and H. Ohno, "A perpendicular-anisotropy CoFeB-MgO magnetic tunnel junction," Nat. Mater. **9**(9), 721–724 (2010).
[10]S. S. P. Parkin, C. Kaiser, A. Panchula, P. M. Rice, B. Hughes, M. Samant, and S.-H. Yang, "Giant tunneling magnetoresistance at room temperature with MgO (100) tunnel barriers," Nat. Mater. **3**(12), 862–867 (2004).
[11]X. Liu, "Thermal stability of magnetic tunneling junctions with MgO barriers for high temperature spintronics," Appl. Phys. Lett. **89**(2), 023504 (2006).
[12]H. Sato, M. Yamanouchi, K. Miura, S. Ikeda, R. Koizumi, F. Matsukura, and H. Ohno, "CoFeB thickness dependence of thermal stability factor in CoFeB/MgO perpendicular magnetic tunnel junctions," IEEE Magn. Lett. **3**, 3000204 (2012).

[13]H. Sato, M. Yamanouchi, K. Miura, S. Ikeda, H. D. Gan, K. Mizunuma, R. Koizumi, F. Matsukura, and H. Ohno, "Junction size effect on switching current and thermal stability in CoFeB/MgO perpendicular magnetic tunnel junctions," Appl. Phys. Lett. **99**, 042501 (2011).
[14]M. Gajek, J. J. Nowak, J. Z. Sun, P. L. Trouilloud, E. J. O'Sullivan, D. W. Abraham, M. C. Gaidis, G. Hu, S. Brown, Y. Zhu *et al.*, "Spin torque switching of 20 nm magnetic tunnel junctions with perpendicular anisotropy," Appl. Phys. Lett. **100**, 132408 (2012).
[15]J. Hong, A. Hadjikhani, M. Stone, F. I. Allen, V. Safonov, P. Liang, J. Bokor, and S. Khizroev, "The physics of spin transfer torque switching in magnetic tunneling junctions in sub-10-nm size range," IEEE Trans. Magn. **52**, 1400504 (2016).
[16]J. Hong, P. Liang, V. L. Safonov, and S. Khizroev, "Energy-efficient spin-transfer torque magnetization reversal in sub-10-nm magnetic tunneling junction point contacts," J. Nanopart. Res. **15**, 1599 (2013).
[17]K. Watanabe, B. Jinnai, S. Fukami, H. Sato, and H. Ohno, "Shape anisotropy revisited in single-digit nanometer magnetic tunnel junctions," Nat. Commun. **9**, 663 (2018).
[18]N. Perrissin, S. Lequeux, N. Strelkov, L. Vila, L. D. Buda-Prejbeanu, S. Auffret, R. C. Sousa, I. L. Prejbeanu, and B. Dieny, "A highly thermally stable sub-20 nm magnetic random-access memory based on perpendicular shape anisotropy," R. Soc. Chem. **10**(25), 12187 (2018).
[19]B. Lee, J. Hong, N. Amos, I. Dumer, D. Litvinov, and S. Khizroev, "Sub-10-nm-resolution electron-beam lithography toward very-high-density multilevel 3D nano-magnetic information devices," J. Nanopart. Res. **15**, 1665 (2013).
[20]J. K. W. Yang, Y. Chen, T. Huang, H. Duan, N. Thiyagarajah, H. K. Hui, S. H. Leong, and V. Ng, "Fabrication and characterization of bit-patterned media beyond 1.5 Tbit/in^2," Nanotechnology **22**(38), 385301 (2011).
[21]H. Shin, S. Hong, J. Moon, and J. U. Jeon, "Read/write mechanisms and data storage system using atomic force microscopy and MEMS technology," Ultramicroscopy **91**, 103–110 (2002).
[22]D.-K. Min and S. Hong, "Servo and tracking algorithm for a probe storage system," IEEE Trans. Magn. **41**(2), 855–859 (2005).
[23]M. Tsoi, A. G. M. Jansen, J. Bass, W. C. Chiang, M. Seck, V. Tsoi, and P. Wyder, "Excitation of a magnetic multilayer by an electric current," Phys. Rev. Lett. **80**, 4281–4284 (1998).
[24]P.-J. Hsu, A. Kubetzka, A. Finco, N. Romming, K. von Bergmann, and R. Wiesendanger, "Electric-field-driven switching of individual magnetic skyrmions," Nat. Nanotechnol. **12**, 123–126 (2017).
[25]J. Hong, M. Stone, B. Navarrete, K. Luongo, Q. Zheng, Z. Yuan, K. Xia, N. Xu, J. Bokor, L. You, and S. Khizroev, "3D multilevel spin transfer torque devices," Appl. Phys. Lett. **112**, 112402 (2018).